

Charge transfer on the metallic atom-pair bond, and the crystal structures adopted by intermetallic compounds

T. Rajasekharan^{a*} and V. Seshubai^b^aDefence Metallurgical Research Laboratory, Kanchanbagh, Hyderabad 500 058, India, and^bSchool of Physics, University of Hyderabad, Hyderabad 500 046, India. Correspondence e-mail: trajasekharan@gmail.com

It has been argued in our recent papers that the heat of formation of intermetallic compounds is mostly concentrated in the nearest neighbor unlike atom-pair bonds, and that the positive term in Miedema's equation is associated with charge transfer on the bond to maintain electroneutrality. In this paper, taking examples of some well populated crystal-structure types such as MgCu₂, AsNa₃, AuCu₃, MoSi₂ and SiCr₃ types, the effect of such charge transfer on the crystal structures adopted by intermetallic compounds is examined. It is shown that the correlation between the observed size changes of atoms on alloying and their electronegativity differences is supportive of the idea of charge transfer between atoms. It is argued that the electronegativity and valence differences need to be of the required magnitude and direction to alter, through charge transfer, the elemental radius ratios R_A/R_B to the internal radius ratios r_A/r_B allowed by the structure types. Since the size change of atoms on alloying is highly correlated to how different R_A/R_B is from the ideal radius ratio for a structure type, the lattice parameters of intermetallic compounds can be predicted with excellent accuracy knowing R_A/R_B . A practical application of the approach developed in our recent papers to superalloy design is presented.

© 2012 International Union of Crystallography
Printed in Singapore – all rights reserved

1. Introduction

Since the advent of the X-ray diffraction technique, a vast amount of data has accumulated on the crystal structures adopted by intermetallic compounds. Theoretical prediction of these structures has interested many workers for a long time. Various reasons have been attributed in the literature to the choice of particular crystal structures by intermetallic compounds: they include geometrical factors, electronic factors and Brillouin zone effects, or a combination thereof (Pearson, 1972, pp. 51–134). Many rules have been formulated using constructs such as metallic radii of atoms, valence electron concentration *etc.* for this purpose (Sauthoff, 1996; Pearson, 1968; Hume Rothery & Raynor, 1954). Structural maps have been constructed using coordinates derived from empirical parameters or quantities derived from pseudo-potential calculations in an attempt to group compounds with different crystal structures in different areas on the maps (Darken & Gurry, 1953; Mooser & Pearson, 1959; Pearson, 1962; St John & Bloch, 1974; Watson & Bennett, 1978; Zunger, 1980; Machlin & Loh, 1980; Pettifor, 1986; Villars & Hulliger, 1987). *Ab initio* techniques have been used to identify the correct crystal structure of an intermetallic compound from several candidate structures, and to obtain their lattice parameters (van de Walle *et al.*, 2007). In this paper we show that

size changes of metallic atoms of alloying are correlated to the direction and magnitude of electronegativity and valence differences between the atoms. Pauling (1950) had proposed charge transfer on the metallic atom-pair bond on alloying, proportional to the electronegativity difference between the atoms, for maintaining electroneutrality. We observe in this paper that the electronegativity differences between atoms in binary intermetallic compounds are of the required magnitude and direction to bring the metallic radii ratio of the elements R_A/R_B , by possible charge transfer, to a value r_A/r_B suitable for ideal packing in their respective crystal structures. Thus, for a particular crystal structure to be adopted by an intermetallic compound, the electronegativity and valence differences between unlike atoms have to be of appropriate magnitude and sign so as to facilitate the size change.

2. The atom-pair bond

Lewis (1916) first proposed that a valence bond in chemical compounds is caused by a shared pair of electrons, one from each atom of the bond. Heitler & London (1927) explained the valence bond quantum-mechanically; they showed that it could be due to the binding of a pair of electrons, one from each atom, by Heisenberg's exchange interaction. An important property of the atom-pair bond is that it is local, and does

not depend much on which atoms or groups of atoms are attached to the end atoms of the bond (Jolly, 1991, p. 62). In his study of chemical bonding, Pauling (1975, pp. 79–91) used the fact that this pair bond can be taken from one substance to another with its strength, length *etc.* remaining unaltered. He combined the idea of pair-bond formation as above with the idea of resonance to explain qualitatively the structure of most organic and metal-organic molecules and most insulating solids. Pauling was able to parameterize the electronic quantities on which the bonding depends and thus quantified most of chemistry (Pauling, 1975; Anderson, 2008). An alternative approach to understanding the bonding in molecules and solids is the molecular-orbital theory (Jolly, 1991, pp. 97–116): one treats the electrons as shared among all the atoms of the molecule or solid, calculating a set of electronic states or molecular orbitals. A linear combination of atomic orbitals (LCAO) approach is commonly used, the justification being that the electrons spend part of their time on each of the atomic orbitals. Calculations using molecular-orbital theory reveal the accumulation of negative charges in the regions between the atoms on the bonds to an extent sufficient to balance the nuclear repulsion forces (Jolly, 1991, pp. 97–116). The amount of electron density that moves into the overlap region is quite small, typically about 0.1 to 0.3 of an electron. Since the charge flow involved is quite small, experimental evidence for the same was scanty earlier. However, accurate X-ray and neutron diffraction data yield good electron density difference maps that show essentially the same sort of information as given by theoretically calculated maps (Jolly, 1991, pp. 97–116). Quantitative measurements of the excess electron density in the bonding region of various carbon–carbon bonds show that the excess ‘bonding charge’ is correlated with the C–C bond length (Jolly, 1991, pp. 97–116). The center of gravity of the charge distribution on an atom-pair bond can be expected to be shifted towards the more electronegative atom; this leaves the less electronegative atom positively charged. An isolated molecule can adopt a conformation that avoids like charges in the neighborhood; but in a metallic solid there should be a charge transfer from the more electronegative atom to the less electronegative one to establish electro-neutrality (Pauling, 1950).

Rajasekharan & Girgis (RG) (1983*a,b*) observed that binary systems with intermetallic compounds of the same crystal structure occur on a straight line (referred to herein as the RG line of the structure type) on a $(\Delta\varphi, \Delta N^{1/3})$ map; φ and N are Miedema’s parameters. φ is proportional to Pauling’s electronegativity χ , and values of N are obtained from the experimental bulk modulus values of elements (Miedema *et al.*, 1975, 1980; Miedema, 1992; Boom *et al.*, 1976). Both parameters φ and N were adjusted numerically by small amounts to accurately predict the signs of the heats of formation of binary metallic systems, using Miedema’s equation given below,

$$\Delta H = f(c) \left[-(\Delta\varphi)^2 + (Q/P)(\Delta N^{1/3})^2 - (R/P) \right]. \quad (1)$$

In a binary system $A-B$, irrespective of whether we consider compounds occurring at AB , AB_2 , AB_3 or in general any A_mB_n , the structures of the concomitant phases are predicted by a knowledge of which RG lines or inverse RG lines pass through the point corresponding to that binary system on the $(\Delta\varphi, \Delta N^{1/3})$ map (Rajasekharan & Seshubai, 2010*a*). This property can be used to predict concomitant and mutually exclusive structure types in binary metallic phase diagrams with excellent reliability (Rajasekharan & Girgis, 1983*a,b*; Rajasekharan & Seshubai, 2010*a*; Kameswari *et al.*, 2010; Kameswari, 2008). These surprising observations were unexplained. It has been argued elsewhere (Rajasekharan & Seshubai, 2010*a*) that the ability of the RG map to predict concomitant structure types in metallic binary systems shows that the energy corresponding to each point on the map is proportional to the energy of the nearest neighbor unlike the atom-pair bond in the intermetallic compounds in question. The energy of the pairwise interaction between A and B atoms, or the $A-B$ bond energy, remains the same for all stoichiometry and structures involved in a binary system (Rajasekharan & Seshubai, 2010*a*). Also, in support of the equivalence in energy of the nearest-neighbor atom-pair bonds in different compounds of the same binary system, it was shown (Rajasekharan & Seshubai, 2010*a*) that in all the 43 binary systems in which $MgCu_2$ -type and $CaCu_5$ -type compounds coexist, the ratio of the shortest $A-B$ bond lengths in the two compounds is uniformly close to 1. Such an effect was also demonstrated (Rajasekharan & Seshubai, 2010*a*) for all the 33 binary systems in which $MgCu_2$ - and $CsCl$ -type compounds co-exist. We thus see that the pair bond in metals can also be taken from one substance to another without its strength or length being altered. Further arguments in favor of the contentions in this paragraph can be seen elsewhere (Rajasekharan & Seshubai, 2010*a*), and are not repeated here.

The pair bonds in intermetallic compounds can be visualized roughly from the unit cell of $MoSi_2$ -type compounds,

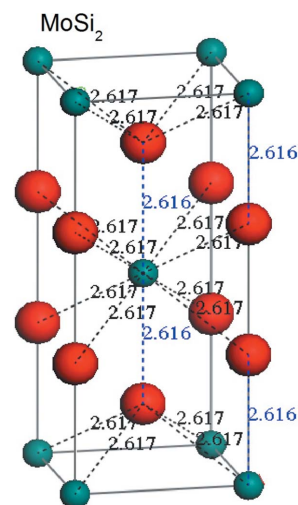


Figure 1

The unit cell of $MoSi_2$ -type (AB_2 , $I18$) compounds. The A atoms are shown as green and the B atoms are shown as red. Several $A-B$ bonds of equal length can be seen in the prototype $MoSi_2$ compound.

shown as a typical example in Fig. 1. An abundance of $A-B$ pairs of equal length can be observed, which allows the small number of electrons available in the metallic system an opportunity to resonate among a large number of equivalent states. A single atom-pair bond can be thought of as an average of such equivalent bonds.

In a recent paper, Rajasekharan & Seshubai (2010*b*) had shown that an expression can be derived for the energy of an atom-pair bond in a metallic alloy in terms of the same average properties of elements, *viz.* electronegativity and valence, which Pauling had used to quantify the whole of chemistry except that of metallic systems. In their paper, Miedema's parameters φ and N were identified as the electronegativity and valence of metallic elements. The negative (stabilizing) contribution to the bond energy had its origin in the ionicity in the bond. The charge transfer on the bond, suggested by Pauling (1950) to establish electroneutrality, contributes the positive term which was quantified in the paper. The paper could explain Miedema's empirically derived equation which predicts the signs of the heats of formation of metallic alloys with 100% accuracy. The value of Miedema's empirically derived constant $(Q/P)^{1/2}$ and the origin of the R/P term followed from the model. It was shown that the energies of the atom-pair bond, calculated using the model for compounds of $MgCu_2$ structure type, are directly correlated to the experimental heats of formation of the compounds; and this fact enables the prediction of the heats of formation values for new compounds of the same structure type. Since the experimental heats of formation of intermetallic compounds can be deduced from the energy of the pair bonds calculated as above, it is clear that most of the energy of the compounds is concentrated in the pair bonds. This conclusion is in agreement with the results of some *ab initio* calculations; pair potential calculations in simple metallic alloys and transition metal alloys have shown that the nearest-neighbor pair interaction energy is more important than the further-neighbor interactions (Machlin, 1986).

As discussed earlier, one of the expected characteristics of the localized atom-pair bond in a metallic alloy is the charge transfer on the bond; this charge transfer can be expected to increase proportional to the electronegativity difference ($\Delta\chi$) between the atoms. We have argued elsewhere (Rajasekharan & Seshubai, 2010*b*) that $\Delta N^{1/3}/2$ is the charge transfer on the atom-pair bond. $\Delta N^{1/3}/2$ has values in the range 0 to 0.5, which is in the same range as the experimental and theoretical estimates (Jolly, 1991, pp. 97–116) of the number of electrons that move into the overlap region.

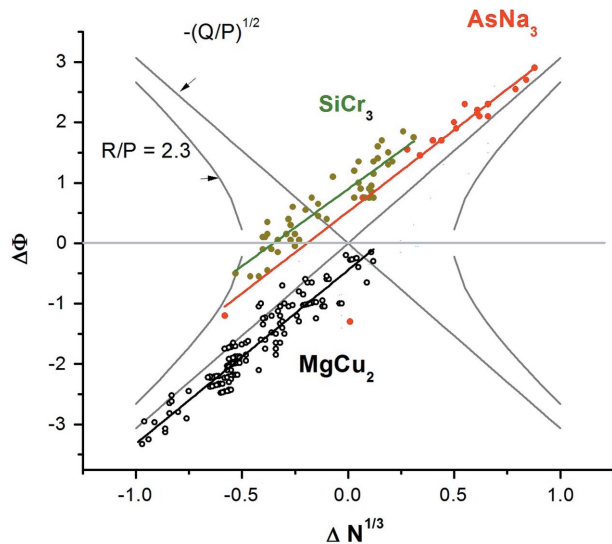
An atom absorbing electrons would become smaller in size owing to the increased attraction of the electron cloud by the nucleus, and the one losing electrons would become larger (Pauling, 1987). In a physical picture where most of the heat of formation of intermetallic compounds is concentrated in the nearest neighbor unlike the atom-pair bond, we might expect that most of the volume changes on alloying should be associated with the charge transfer on the bond. It might be anticipated that such charge transfer plays a crucial role in deciding the crystal structures and lattice parameters of

intermetallic compounds. We verify these propositions taking some examples of well populated structure types in the subsequent sections of this paper. We have described the structure types considered in this paper only briefly; more details can be found elsewhere (Pearson, 1972). The crystallographic data are from standard sources (Pearson, 1967; Villars & Calvert, 1985; Massalski, 1990).

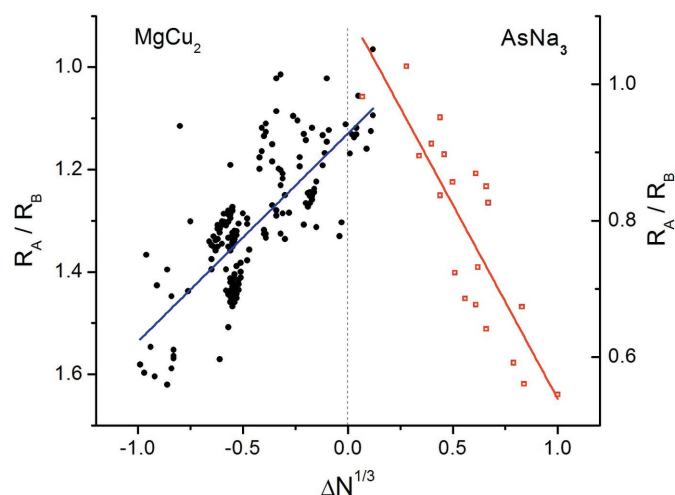
3. Charge transfer on the atom-pair bond, and size changes during alloying

The binary Laves phases with an AB_2 composition belong to the topologically close-packed (TCP) structures (Pearson, 1972, p. 654). In the group of TCP intermetallics, Laves phases constitute the largest group. They crystallize in the hexagonal C14 (*hP12*, $MgZn_2$ prototype), the cubic C15 (*cF24*, $MgCu_2$ prototype) or the dihexagonal C36 (*hP24*, $MgNi_2$ prototype) structures. The C14, C15 and C36 structures differ only by the particular stacking of the same two-layered structural units (Hazzledine *et al.*, 1993). The stability of these structure types has been proposed to be controlled by both the atomic size ratio of the A and B atoms and the valence electron concentration (Sauthoff, 1996). We consider in this paper the C15 $MgCu_2$ -type compounds as the first illustrative example. Approximately 180 binary compounds are known which crystallize with the $MgCu_2$ -type structure. An atom of diameter $D = 2R$ in the metallic element will have a different diameter $d = 2r$ in a Laves phase. The atomic size difference between the metallic (elemental) and intermetallic phases ($D - d$) yields an apparent contraction or expansion of an atom within a Laves phase. For C15, assuming a hard sphere model, $d_{AA} = 3^{1/2}a/4$, $d_{BB} = 2^{1/2}a/4$, $d_{AB} = 11^{1/2}a/8$. d_{AA} is the distance between two A atoms in the structure, which is considered equal to the $A-A$ bond length. Similarly, d_{BB} is the $B-B$ distance and d_{AB} is the $A-B$ distance. a is the lattice parameter. The compounds occur with the ratio of metallic radii in the range $R_A/R_B = 1.05-1.68$. The atoms forming the compounds need to adjust in size to accommodate the ideal size filling ratio $r_A/r_B = 1.225$ in the ordered Laves phase lattice; as a result, the occurrence of Laves phases is related to the ability of the A and B atoms to change size so that the ideal ratio is approached. Mechanical stresses have been assumed to explain such size changes (Pearson, 1972, p. 52; Pearson, 1968). Another possible mechanism is charge transfer between the atoms on alloying. A systematic dependence of the size changes of atoms on alloying on their electronic properties, *i.e.* electronegativity and valence differences, might be considered as supportive of the latter mechanism.

The $AsNa_3$ -type compounds are hexagonal, *hP8* (Pearson, 1967). Pearson (1972, p. 654) had noticed that the dimensional behavior of the phases is controlled by the six Na (II) neighbors surrounding each As atom. Unlike the $NiAs$ -type compounds, which occur with widely varying axial ratios, the 19 known phases with the $AsNa_3$ -type structure are remarkable for the constancy of their axial ratio which has a value of 1.79 ± 0.03 . In Fig. 2 the RG lines of $AsNa_3$ and $MgCu_2$ -type structures can be seen in the first and third quadrants,


Figure 2

The RG lines of MgCu_2 , AsNa_3 and SiCr_3 crystal-structure types. The binary systems in which compounds of these crystal structures occur are plotted on a $(\Delta\phi, \Delta N^{1/3})$ map. $\Delta\phi = (\varphi_A - \varphi_B)$ and $\Delta N^{1/3} = (N_A^{1/3} - N_B^{1/3})$, where A is the minority element. Binary systems with compounds belonging to each structure type fall on a straight line on the map. From the overlap and lack of overlap between the lines, one can predict concomitant and mutually exclusive structure types in binary systems (Rajasekharan & Seshubai, 2010*a*). Most of the compounds of the MgCu_2 -type crystal structure have negative $\Delta\phi$, and most of the compounds with SiCr_3 and AsNa_3 -type structures have positive $\Delta\phi$.

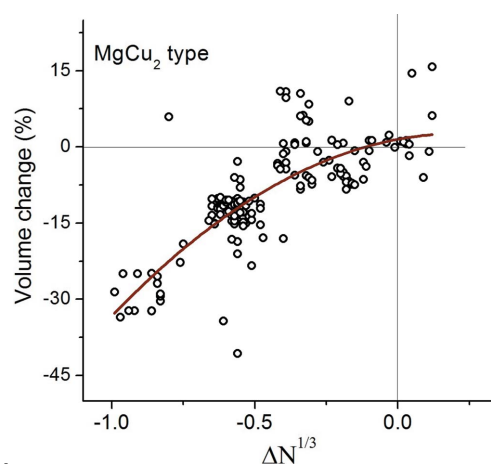

Figure 3

R_A/R_B is plotted versus $\Delta N^{1/3}$ for MgCu_2 and AsNa_3 -type compounds. Compounds exist in both systems over a wide range of R_A/R_B values. No preference is shown for any particular metallic radii ratios. A is the minority element. R_A and R_B are the radii of the atoms in the elemental state. $\Delta N^{1/3} = N_A^{1/3} - N_B^{1/3}$ is negative for MgCu_2 -type compounds and so is $\Delta\phi = \varphi_A - \varphi_B$. $\Delta\phi \propto \Delta N^{1/3}$ for the compounds as can be seen from Fig. 2. The direction of charge transfer has to be from the more electronegative atom to the less electronegative atom according to Pauling (1950), *i.e.* from B to A , and the A atoms become smaller owing to the enhanced attraction by the positive charges at the core. The radius ratios of the atoms shift from R_A/R_B which are in the range above 1.0 to values suitable for ideal packing in the MgCu_2 -type structure. The maximum change in radii is for compounds with $R_A/R_B \gg 1$ and with $|\Delta N^{1/3}| \simeq 1$; the minimum change is when $R_A/R_B \simeq 1.0$ at $|\Delta N^{1/3}| \simeq 0$. The variation of R_A/R_B with $\Delta N^{1/3}$ is almost linear. A similar argument will show that radii ratios will shift from R_A/R_B values which are in the range less than 1.0 for AsNa_3 -type compounds, to values close to 1.0 by charge transfer.

respectively, on the $(\Delta\phi, \Delta N^{1/3})$ map. Nineteen binary systems with AsNa_3 -type (AB_3) and 181 binary systems with MgCu_2 -type (AB_2) compounds are considered. We note that all the AsNa_3 -type compounds have their $\Delta\phi (= \varphi_A - \varphi_B)$ and $\Delta N^{1/3} (= N_A^{1/3} - N_B^{1/3})$ values positive. MgCu_2 -type compounds have their $\Delta\phi (= \varphi_A - \varphi_B)$ and $\Delta N^{1/3} (= N_A^{1/3} - N_B^{1/3})$ values negative. Here, A is the minority element. In Fig. 3 we plot R_A/R_B versus $\Delta N^{1/3}$ for the MgCu_2 - and AsNa_3 -type compounds. We see that compounds exist in both systems with a wide range of R_A/R_B values. No preference is shown for $R_A/R_B = 1.225$ by the MgCu_2 -type compounds and for any particular R_A/R_B value by the AsNa_3 -type compounds. The R_A/R_B values deviate maximally from ~ 1.0 at $|\Delta N^{1/3}| \simeq 1$, and vary to a value of ~ 1.0 at $|\Delta N^{1/3}| \simeq 0$. The variation of R_A/R_B with $\Delta N^{1/3}$ is almost linear. For MgCu_2 -type compounds, $N_A^{1/3} < N_B^{1/3}$ and $\varphi_A < \varphi_B$. According to Pauling's model, charge is transferred from the more electronegative element to the less electronegative one, and the latter would decrease in diameter. The effect of charge transfer is to decrease the radius ratios of the atoms from the metallic radii ratio $R_A/R_B > 1$ to the ideal size filling ratio r_A/r_B which is close to 1. We observe from Fig. 3 that $|\Delta N^{1/3}|$, and thus the amount of charge transfer, increases in proportion to the deviation of R_A/R_B from 1.0. In Fig. 4 we show the change in volume on alloying as a function of $\Delta N^{1/3}$ for MgCu_2 -type compounds; we observe that the volume change goes to zero when $\Delta N^{1/3}$ goes to zero.

A similar argument will show that the effect of charge transfer in AsNa_3 -type compounds is to increase the internal radius ratio towards 1.0 by charge transfer. The greater the deviation of R_A/R_B from 1, the greater is the charge transfer $\Delta N^{1/3}/2$.

Another interesting example is the case of MoSi_2 -type compounds. MoSi_2 -type compounds (Pearson, 1972, p. 589)


Figure 4

Percentage change in volume on alloying as a function of $\Delta N^{1/3}$ for MgCu_2 -type compounds. The volume per molecule estimated from the molar volumes of the elements is subtracted from the volume per molecule computed from the unit-cell volumes of the compounds, and expressed as a percentage relative to the volume per molecule before alloying. It can be observed that the change in volume goes to zero when $\Delta N^{1/3}$ goes to zero. This observation supports the idea that $\Delta N^{1/3}$ is proportional to the charge transfer on alloying.

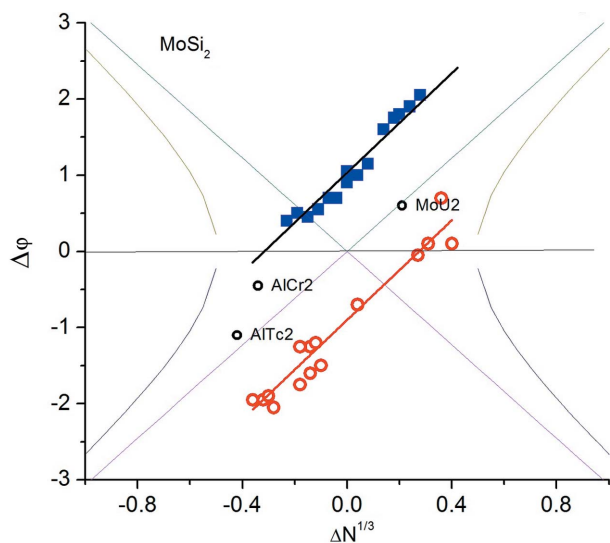


Figure 5 Binary systems with MoSi₂-type compounds occur on two straight lines on the ($\Delta\phi$, $\Delta N^{1/3}$) map. AlCr₂, AlTc₂ and MoU₂ (black open circles) are exceptions. *A* is the minority element. Blue squares represent compounds with $\Delta\phi = \varphi_A - \varphi_B$ positive and red open circles represent compounds with $\Delta\phi = \varphi_A - \varphi_B$ negative.

are tetragonal, *tI8*. It is known that there are two groups of compounds of the MoSi₂-type structure. One group has larger axial ratio (*c/a*) values, and the other, smaller. It can be seen from Fig. 5 that the 37 binary systems with MoSi₂-type compounds form two RG lines with the compounds AlTc₂, AlCr₂ and MoU₂ as exceptions. We see from Fig. 6, in which *c/a* is plotted versus R_A/R_B , that the compounds in Fig. 5 are resolved as per their axial ratios. The same compounds AlTc₂, AlCr₂ and MoU₂ are exceptions in both the figures. The R_A/R_B values go to 1.0 on both the lines as $\Delta N^{1/3}$ goes to zero. The upper line in Fig. 5 has the same compounds as the lower line in Fig. 6: it has compounds with $R_A/R_B > 1$ and with lower *c/a* values. The direction of charge transfer in the compounds on both the lines in Fig. 5, as given by the sign of $\Delta\phi$, is such as to alter the R_A/R_B values towards the internal radius ratio $r_A/r_B \simeq 1$ of the structure type. The magnitude of $\Delta\phi$ is proportionally larger when R_A/R_B deviates more from 1.0. We can define $R_A - r_A$ as the change in radius of minority *A* atoms on alloying, where r_A is the radius of the atom in the alloy. In Fig. 7 we plot $R_A - r_A$ versus R_A/R_B for MoSi₂-type compounds. r_A is calculated from the lattice parameters of the compounds as $r_A = 0.5[(a^2/2) + (c^2/36)]^{1/2}$. We observe from Fig. 7 that $|R_A - r_A|$, which is almost zero at $R_A/R_B = 1$, increases proportionately as R_A/R_B deviates from 1. We also observe that the increase or decrease in the sizes of the atoms is consistent with Pauling's hypothesis on which of the atoms would give up or gain electrons based on the electronegativity difference between the atoms. In Fig. 8 we plot the change in volume when MoSi₂-type compounds form from their constituent elements, as a function of $\Delta N^{1/3}$. The change in volume goes to zero when $\Delta N^{1/3}$ goes to zero.

We consider another example: *viz.* the L1₂ (AuCu₃) structure type. There are about 240 compounds with this structure (Pearson, 1967), which includes Ni₃Al. It is cubic (*cP4*) with

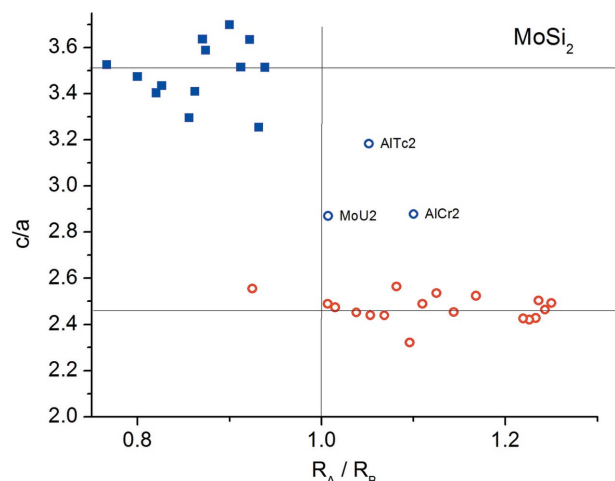


Figure 6 On a plot of *c/a* versus R_A/R_B , the MoSi₂-type compounds form two groups. AlCr₂, AlTc₂ and MoU₂ (blue open circles) which were exceptions in Fig. 5 are exceptions in this figure too. The compounds with $\Delta\phi = \varphi_A - \varphi_B$ positive (blue squares) have higher *c/a* values and have R_A/R_B values less than 1.0. The direction of charge transfer (Pauling, 1950) is appropriate to shift the radius ratio of the atoms to 1.0 in the structure. The compounds with $\Delta\phi = \varphi_A - \varphi_B$ negative (red open circles) have lower *c/a* values and have R_A/R_B values greater than 1.0. The direction of charge transfer is appropriate to shift the radius ratio of the atoms to 1.0 in the structure.

the minority atoms (*A*) at the corners of the unit cell, and the majority atoms (*B*) ordered in the face centers. We can define $R_A - r_A$ as the change in radius of the minority atoms on alloying, where r_A is the radius of atom *A* in the alloy. For AuCu₃-type structure, $r_A = a/[2(2^{1/2})]$, where *a* is the lattice parameter of the compound. In Fig. 9 we show a plot of $R_A - r_A$ versus R_A/R_B for the 240 AuCu₃-type compounds. The graph can be fitted to the equation $R_A - r_A = 2.313 +$

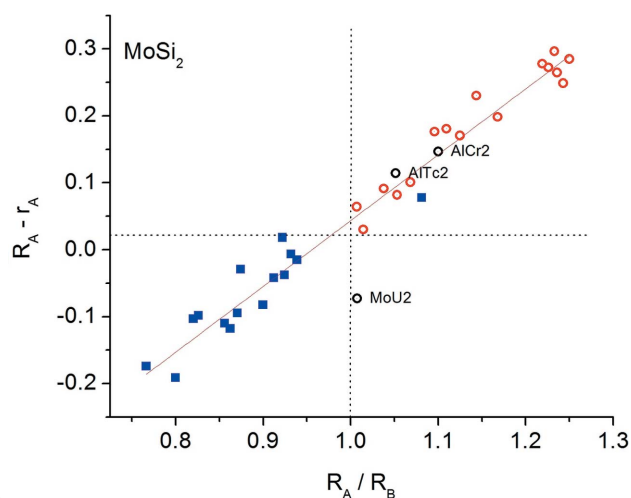
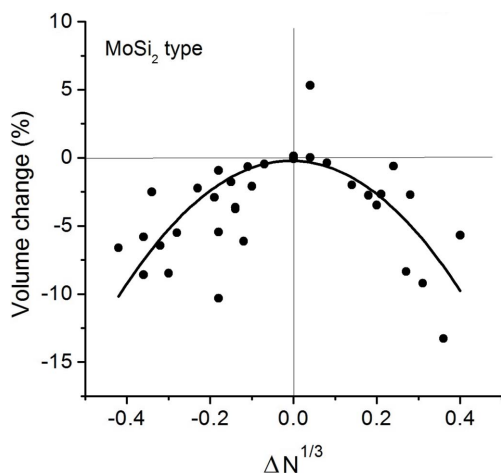
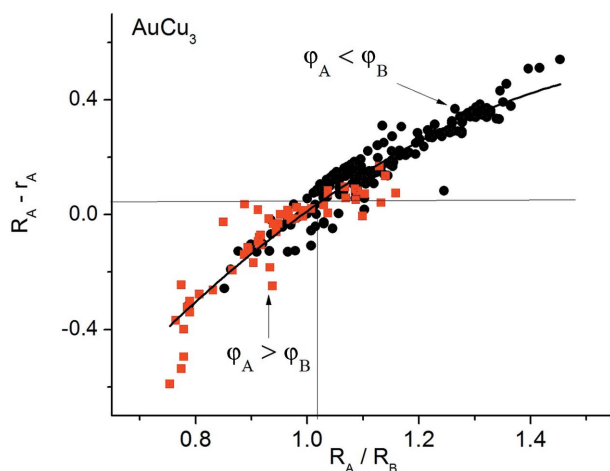


Figure 7 Change in radius of the minority atom on alloying *i.e.* $R_A - r_A$ is plotted versus R_A/R_B for MoSi₂-type compounds. r_A is the radius of the *A* atom in the structure and is calculated from the lattice parameters as $0.5[(a^2/2) + (c^2/36)]^{1/2}$. The plot is linear and $R_A - r_A$ is almost zero when $R_A/R_B = 1$. The compounds with $\Delta\phi = \varphi_A - \varphi_B$ positive (blue squares) have $R_A - r_A$ negative, and $|R_A - r_A|$ increases with the deviation of R_A/R_B from 1. The compounds with $\varphi_A - \varphi_B$ negative (red open circles) have r_A decreasing with increasing R_A/R_B .

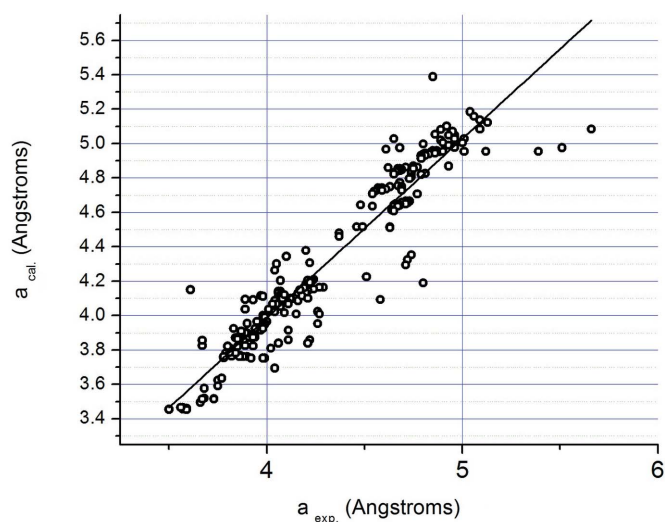

Figure 8

Percentage change in volume on alloying as a function of $\Delta N^{1/3}$ for MoSi_2 -type compounds. The volume per molecule estimated from the molar volumes of the elements is subtracted from the volume per molecule computed from the unit-cell volumes of the compounds, and expressed as a percentage relative to the volume per molecule before alloying. It can be observed that the change in volume goes to zero when $\Delta N^{1/3}$ goes to zero. This observation supports the idea that $\Delta N^{1/3}$ is proportional to the charge transfer on alloying.

$3.255(R_A/R_B) - 0.929(R_A/R_B)^2$. There are a few compounds which deviate from the curve at its ends; the deviations (~ 9 out of 240) are probably related to their large $|R_A/R_B|$ values which make them behave like interstitial compounds. The compounds for which $\varphi_A > \varphi_B$ are marked by full squares (red online) and those for which $\varphi_A < \varphi_B$ are marked by full circles (black online). In AuCu_3 -type compounds the best space filling of 74% is expected (Pearson, 1972) when $R_A/R_B = 1$. When $\varphi_A > \varphi_B$ we expect charge to be transferred from A to B


Figure 9

Plot of the change in radius of the minority atom on alloying $R_A - r_A$ versus R_A/R_B for 240 AuCu_3 -type compounds. r_A is the radius of the A atom in the structure and is calculated from the lattice parameter as $a/[2(2^{1/2})]$. The points can be fitted to the equation $R_A - r_A = 2.313 + 3.255(R_A/R_B) - 0.929(R_A/R_B)^2$. $R_A - r_A$ is almost zero when $R_A/R_B = 1$. The compounds with $\varphi_A > \varphi_B$ (red squares) have $R_A - r_A$ negative, and those with $\varphi_A < \varphi_B$ (black circles) have $R_A - r_A$ positive. The change in size of the atoms is in accordance with the hypothesis that the more electronegative atoms transfer electrons to the less electronegative ones on alloying.


Figure 10

Plot of the lattice parameters of 240 AuCu_3 -type compounds, calculated using the correlation observed in Fig. 9, versus the experimentally observed values. One observes that lattice parameters of new compounds can be predicted with reasonable accuracy starting with the elemental radius ratios.

making atom A larger and atom B smaller. $R_A - r_A$ would be negative in such cases. We note that in such cases the radius ratio r_A/r_B after charge transfer increases to 1.0 (from R_A/R_B values less than 1), thus allowing for maximum space filling. In cases where $\varphi_A < \varphi_B$, the charge transfer would be from B to A , and would make the internal radius ratio approach 1 from R_A/R_B values which are larger than 1. The correlation in Fig. 9 allows the lattice parameters of new L_{12} compounds to be predicted with reasonable accuracy. This aspect is illustrated in Fig. 10 where we compare the calculated and observed lattice parameters of 240 compounds of AuCu_3 -type structure.

In intermetallic compounds, a liganacy ≥ 8 is generally observed (Laves, 1966). Assuming spherical atoms or ions, for ideal packing with liganacy ≥ 8 , the internal radius ratio r_a/r_b has to be between 0.732 and 1.0 (Pauling, 1929). The observations of this paper show that the size changes of atoms on intermetallic compound formation are correlated to the magnitude and sign of the electronegativity differences between the atoms. These size changes assure that the high liganacy and coordination numbers observed in intermetallic compounds can be attained. The question of whether a particular crystal structure would be adopted by an intermetallic compound depends on whether its $\Delta\varphi$ and $\Delta N^{1/3}$ are of the correct magnitude and direction on the atom-pair bond to modify the elemental R_A/R_B by charge transfer to a value close to the internal r_A/r_B characteristic of the structure type.

4. The lattice parameters

We will now investigate, with a few more examples, the effect of change in size of the atoms on the atom-pair bond in deciding the lattice parameters of intermetallic compounds. We show a plot of $R_A - r_A$ versus R_A/R_B for 181 MgCu_2 -type

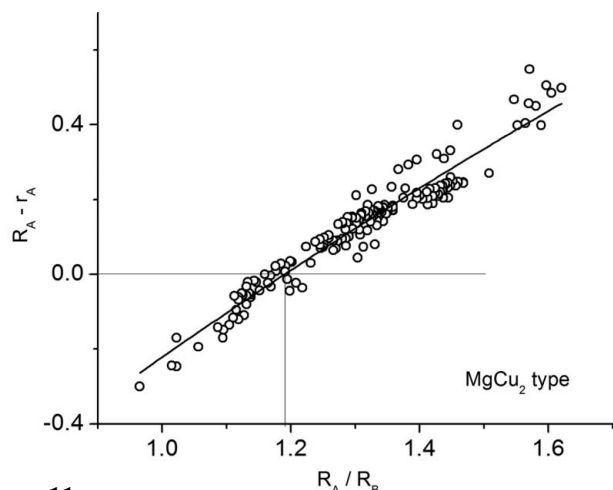


Figure 11
Plot of the change in radius of the minority atom on alloying $R_A - r_A$ versus R_A/R_B for 181 $MgCu_2$ -type compounds. r_A is the radius of the A atom in the structure and is calculated from the lattice parameter as $3^{1/2}a/8$. The points can be fitted to the equation $R_A - r_A = -1.587 + 1.534(R_A/R_B) - 0.168(R_A/R_B)^2$. A systematic deviation is observed for the points at the end of the line as in the case of the $AuCu_3$ -type compounds in Fig. 9. $R_A - r_A$ is almost zero when $R_A/R_B \approx 1.2$, close to the internal radius ratio of 1.225 proposed by Laves (1966).

(AB_2) compounds in Fig. 11. The r_A values were obtained from the unit-cell dimensions as $3^{1/2}a/8$. The plot can be fitted to the equation $R_A - r_A = -1.587 + 1.534(R_A/R_B) - 0.168(R_A/R_B)^2$. There are a few compounds deviating at the ends of the curve as in the case of the $AuCu_3$ -type compounds. The correlation enables one to predict accurately the r_A value of a new compound knowing only its elemental R_A/R_B . Its lattice parameter can then be estimated to a high accuracy using the relation $a = (8/3^{1/2})r_A$. Fig. 12 compares the observed lattice parameters of $MgCu_2$ -type compounds and the ones calculated using the present correlation. We note that in spite of considering all known binary $MgCu_2$ -type compounds, including those in all elemental combinations, the difference

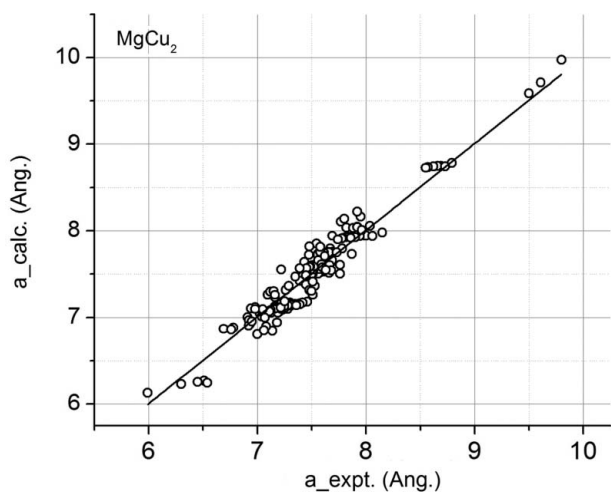


Figure 12
Plot of the lattice parameters 181 $MgCu_2$ -type compounds, calculated using the correlation observed in Fig. 11, versus the experimentally observed values. One observes that lattice parameters of new compounds can be predicted with reasonable accuracy starting with the elemental radius ratios.

Table 1
Experimental lattice parameters of $AsNa_3$ -type compounds along with those calculated using the correlation in Fig. 13.

The differences (Diff.) between the experimental (exp.) and calculated (calc.) values are also given. The lattice parameters are in Å.

No.	Compound	<i>a</i> (exp.)	<i>a</i> (calc.)	<i>c</i> (exp.)	<i>c</i> (calc.)	Diff. in <i>a</i>	Diff. in <i>c</i>
1	HgMg ₃	4.87	4.88	8.66	8.69	0.01	-0.03
2	IrAl ₃	4.25	4.13	7.76	7.36	-0.12	0.40
3	AuMg ₃	4.84	4.64	8.46	8.27	-0.20	0.19
4	AsLi ₃	4.38	4.42	7.80	7.87	0.04	-0.07
5	BiNa ₃	5.46	5.65	9.67	10.07	0.19	-0.40
6	PtMg ₃	4.58	4.51	8.32	8.04	-0.07	0.28
7	PdMg ₃	4.61	4.48	8.41	7.98	-0.13	0.43
8	IrMg ₃	4.55	4.46	8.23	7.95	-0.09	0.28
9	SbNa ₃	5.37	5.42	9.52	9.66	0.05	-0.14
10	PLi ₃	4.27	4.24	7.59	7.55	-0.04	0.05
11	AsNa ₃	5.1	5.07	9.00	9.04	-0.03	-0.04
12	BiK ₃	6.19	6.34	10.96	11.29	0.15	-0.33
13	BiRb ₃	6.42	6.52	11.46	11.62	0.10	-0.16
14	SbK ₃	6.04	6.13	10.71	10.93	0.09	-0.21
15	PNa ₃	4.99	4.92	8.82	8.77	-0.07	0.05
16	SbRb ₃	6.25	6.32	11.12	11.26	0.07	-0.14
17	AsK ₃	5.79	5.80	10.24	10.34	0.01	-0.10
18	AsRb ₃	6.05	5.99	10.73	10.67	-0.06	0.06
19	PK ₃	5.69	5.65	10.05	10.07	-0.04	-0.02

between the experimental and calculated lattice parameter values are minimal.

In systems of lower symmetry, where the axial ratio is more or less a constant, for instance in the $AsNa_3$ -type compounds, we need only one distance to decide approximately both the cell parameters. We have shown an $R_A - r_A$ versus R_A/R_B plot for $AsNa_3$ -type compounds (*hP8*) with 19 representatives in Fig. 13. The r_A values are calculated from the geometry of the structure as $[(a/3^{1/2}) - (12a^2 + c^2)^{1/2}/12]$. The plot has a high regression factor and allows the lattice parameters of new hypothetical compounds with $AsNa_3$ -type structure to be calculated with good accuracy, assuming an average c/a value

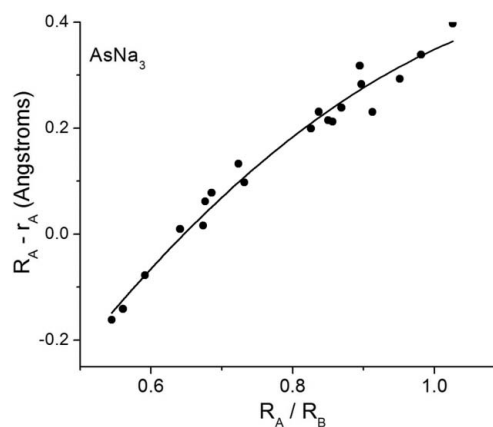


Figure 13
Plot of the change in radius $R_A - r_A$ of the minority atoms on alloying versus R_A/R_B for 19 $AsNa_3$ -type compounds. r_A is the radius of the A atom in the structure and is calculated from the lattice parameters as $r_A = [a/3^{1/2} - (12a^2 + c^2)^{1/2}/12]$. The points can be fitted to an equation $R_A - r_A = -1.308 + 2.693(R_A/R_B) - 1.037(R_A/R_B)^2$. Lattice parameters of new compounds of the same structure type can be estimated with good accuracy from the observed correlation, as demonstrated in Table 1.

Table 2

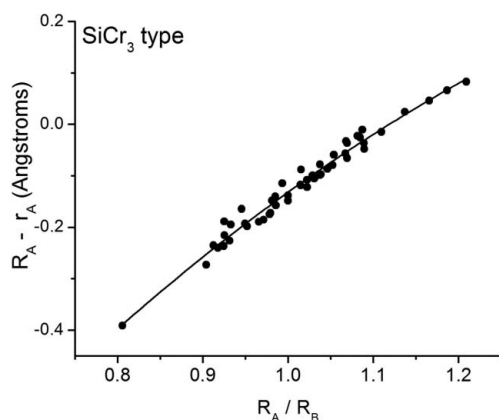
The lattice parameters of 50 SiCr₃-type compounds calculated using the polynomial fit in Fig. 14 are compared with the experimental values.

All elemental combinations with SiCr₃-type compounds are considered. The difference (Diff.) between the calculated (calc.) and experimental (exp.) values is mostly ≤ 0.05 Å. Lattice-parameter values are in Å.

No.	Compound	<i>a</i> (calc.)	<i>a</i> (exp.)	Diff.	No.	Compound	<i>a</i> (calc.)	<i>a</i> (exp.)	Diff.
1	SnV ₃	4.98	4.96	-0.02	26	SiCr ₃	4.56	4.64	0.08
2	SbV ₃	4.93	4.93	0.00	27	IrV ₃	4.79	4.77	-0.02
3	SnMo ₃	5.09	5.09	0.00	28	GaMo ₃	4.94	4.93	-0.01
4	InNb ₃	5.29	5.31	0.02	29	AuNb ₃	5.21	5.15	-0.05
5	SnNb ₃	5.29	5.27	-0.02	30	RhV ₃	4.78	4.76	-0.02
6	AuV ₃	4.88	4.82	-0.06	31	AuTi ₃	5.10	5.18	0.08
7	SbNb ₃	5.26	5.25	-0.02	32	GeMo ₃	4.94	4.92	-0.03
8	SnTa ₃	5.28	5.35	0.07	33	SiV ₃	4.73	4.76	0.03
9	GaCr ₃	4.65	4.68	0.03	34	HgZr ₃	5.56	5.58	0.02
10	SbTi ₃	5.22	5.27	0.05	35	AlNb ₃	5.19	5.13	-0.05
11	AsCr ₃	4.62	4.67	0.05	36	IrMo ₃	4.97	4.91	-0.05
12	PtCr ₃	4.71	4.67	-0.04	37	OsMo ₃	4.97	4.91	-0.06
13	HgTi ₃	5.19	5.25	0.07	38	GaNb ₃	5.18	5.12	-0.05
14	AlV ₃	4.81	4.80	-0.01	39	PtNb ₃	5.14	5.12	-0.02
15	GeCr ₃	4.63	4.66	0.03	40	SiMo ₃	4.90	4.90	0.00
16	GaV ₃	4.82	4.79	-0.03	41	PtTi ₃	5.03	5.14	0.11
17	IrCr ₃	4.68	4.65	-0.03	42	CoV ₃	4.68	4.74	0.07
18	OsCr ₃	4.68	4.65	-0.03	43	IrNb ₃	5.13	5.10	-0.03
19	PtV ₃	4.82	4.78	-0.03	44	NiV ₃	4.71	4.74	0.03
20	AsV ₃	4.75	4.78	0.03	45	IrTi ₃	5.01	5.13	0.12
21	RhCr ₃	4.67	4.65	-0.03	46	OsNb ₃	5.14	5.10	-0.04
22	RuCr ₃	4.68	4.65	-0.03	47	RhNb ₃	5.12	5.10	-0.02
23	AlMo ₃	4.95	4.95	0.00	48	AuZr ₃	5.49	5.51	0.02
24	PdV ₃	4.83	4.77	-0.05	49	SiNb ₃	5.16	5.09	-0.07
25	GeV ₃	4.78	4.77	-0.01	50	BeMo ₃	4.89	4.88	-0.01

of 1.79. In Table 1 we compare the experimental lattice parameters of AsNa₃-type compounds with those calculated from the polynomial fit in Fig. 13.

There are around 50 intermetallic compounds with A15-type (SiCr₃-type, *cP8*) crystal structure. They are an interesting group of compounds since many of them are superconducting. In Fig. 14 we plot $R_A - r_A$ versus R_A/R_B for SiCr₃-type compounds. The r_A values are obtained from the geometry of the structure as $(5^{1/2} - 1)a/4$. The plot has a high regression factor and enables the lattice parameter of a new compound of the same structure type to be calculated with


Figure 14

Plot of the change in radius $R_A - r_A$ of the minority atom on alloying versus R_A/R_B for 50 SiCr₃-type compounds. r_A is the radius of the *A* atom in the structure and is calculated from the lattice parameter as $(5^{1/2} - 1)a/4$. The points can be fitted to an equation $R_A - r_A = -2.002 + 2.544(R_A/R_B) - 0.675(R_A/R_B)^2$. Lattice parameters of new compounds of the same structure type can be estimated with good accuracy from the observed correlation, as demonstrated in Table 2.

a maximum error of ~ 0.05 Å. In Table 2 we compare the experimental lattice parameters of SiCr₃-type compounds with those calculated from the polynomial fit in Fig. 14.

Lattice parameters can be predicted for compounds belonging to several other structure types as well, from the change in radii of the atoms on the atom-pair bond. Lattice parameters can also be obtained for hexagonal NiAs-type (*hP4*) compounds where c/a varies over a wide range: one can determine both a and c using the linear dependences of $R_A - r_A$ and $R_B - r_B$ on R_A/R_B . The atomic radii change on alloying is observed to be uniformly consistent with Pauling's hypothesis on the direction of charge transfer on the atom-pair bond on alloying.

5. Summary

Owing to high symmetry and ligancy, for most crystal-structure types in which intermetallic compounds crystallize, the internal radius ratios of the atoms are close to 1.0. The elemental radius ratios have to change on alloying, to match the internal radius ratios allowed by the structure types. The size changes of atoms on alloying are shown in this paper to be systematically related to the direction and magnitude of the difference in their electronegativity and valence, and to be consistent with the expectations from the picture of charge transfer on the metallic atom-pair bond. It is also shown that the change in radii of the atoms on the nearest-neighbor atom-pair bond predominantly decides the unit-cell dimensions of intermetallic compounds. It is argued that the correlation between the observed size changes of atoms on alloying and

their electronegativity differences is supportive of the idea of charge transfer between atoms on alloying.

It must be emphasized that the basic motivation for a re-examination of the concept of localized covalent bonds in metals is the observation that concomitant and mutually exclusive structure types in metallic binary systems can be predicted using the Rajasekharan–Girgis map. This observation suggested the possibility of defining a bond energy for the metallic atom-pair bond, which does not depend on which atoms or groups of atoms are attached to the end atoms of the bond, just as in conventional chemistry. Further, it was found (Rajasekharan & Seshubai, 2010*b*) that it is possible to predict accurately the signs of the heats of formation of metallic alloys from the energy calculated for the atom-pair bond. The negative (stabilizing) contribution to the energy of the bond resulted from the ionicity in the bonds, and the positive contribution from the charge transfer on the bond to maintain electroneutrality. In this paper we have demonstrated that the size changes of atoms on alloying are supportive of such a charge-transfer mechanism.

It is of interest in the context of the present paper that an *ab initio* application of Pauling’s resonating valence bond (RVB) theory to simpler systems such as Li atom clusters brings out the covalent character of the metal–metal bond and the importance of the metallic orbital (Mohallem *et al.*, 1997). Diffusion quantum Monte Carlo simulations of Li clusters show that RVB pairing correlations between electrons provide a substantial contribution to the cohesive energy (Nissenbaum *et al.*, 2009). Elsewhere (Harcourt & Styles, 2003), valence-bond studies of aspects of electron conduction along a linear chain of lithium atoms have been reported. Marchi *et al.* (2011) have studied the nature of the chemical bond in undoped grapheme through *ab initio* techniques, and have shown that the RVB picture remains valid within a ‘resonance length’ of a few atomic units. Although we have used the ideas of charge transfer and accompanying size changes as propounded by Pauling, it is not proven that the RVB idea has to be invoked to describe the collective nature of bonding in metallic systems. The molecular-orbital theory, employing a combination of atomic orbitals, also gives solutions with excess charge density in the overlap region. This charge density is quite small (0.1–0.3 electrons) and is comparable in magnitude to $\Delta N^{1/3}/2$, which is the charge transfer on the bond according to our model (Rajasekharan & Seshubai, 2010*b*). The electronegativity difference between the atoms can cause the bonding electrons to shift closer to the more electronegative atom, generating a requirement for charge transfer to establish electroneutrality.

The present work throws light on the fundamental interactions in metallic systems. Further, it can be useful for predicting the properties of metallic systems in the laboratory or industry. An example would be superalloy design; one can predict elements which would form coherent L1₂ (AuCu₃-type) precipitates in the Ni matrix of superalloys using the Rajasekharan–Girgis map (see Fig. 15), and judge the coherency of such precipitates with the Ni matrix by calculating their lattice parameters using Fig. 9. It is also interesting to

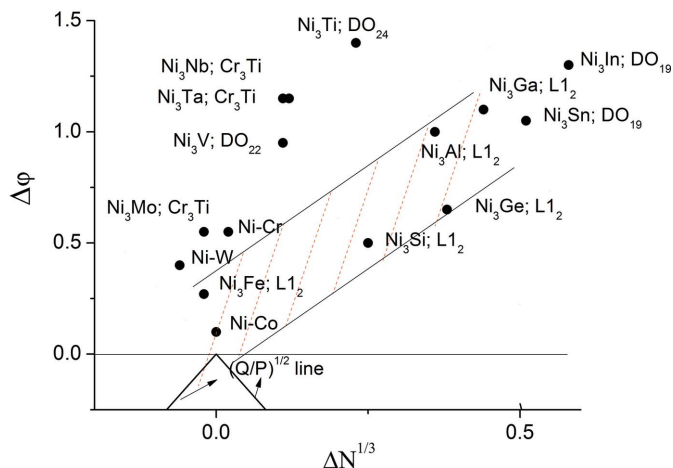


Figure 15 Ni-based binary systems with some alloying elements of interest in superalloy design; $\Delta\phi = (\phi_A - \phi_B)$ and $\Delta N^{1/3} = (N_A^{1/3} - N_B^{1/3})$, where Ni is the element A. We observe that those binary systems in which L1₂ (AuCu₃-type) compounds occur at the composition A₃B occur in a particular region (shaded) of the map. The Ni–Co system, being close to the origin, has low energy in the Ni–Co (atom-pair) bonds and there are no ordered compounds in the system. Ni₃Fe is an L1₂ compound close to the origin; it has a lower ordering temperature of 790 K in comparison with the other L1₂ compounds. The morphology of the AuCu₃-type precipitates in the Ni matrix of superalloys is determined by the mismatch in their lattice parameters with respect to the Ni matrix (Jena & Chaturvedi, 1984). The lattice parameters of the L1₂ compounds can be deduced from Fig. 10.

note that the picture of pairwise interaction in metals and alloys has the potential to be the starting point in techniques such as Monte Carlo or molecular dynamics simulations of metallic systems.

TR thanks DMRL, Hyderabad, India, for permission to publish this paper.

References

- Anderson, P. (2008). *Phys. Today*, **61**, 8–9.
 Boom, R., de Boer, F. R. & Miedema, A. R. (1976). *J. Less Common Met.* **45**, 237–245.
 Darken, L. S. & Gurry, R. W. (1953). *Physical Chemistry of Metals*. New York: McGraw Hill-Education.
 Harcourt, R. D. & Styles, M. L. (2003). *J. Phys. Chem. A*, **107**, 3877–3883.
 Hazzledine, P. M., Kumar, K. S., Miracle, D. B. & Jackson, A. G. (1993). *High Temperature Ordered Intermetallic Alloys V*, edited by I. Baker, R. Darolia, J. D. Whittenberger & M. H. Yoo, Vol. 288, pp. 591–596. Pittsburgh: Materials Research Society.
 Heitler, W. & London, F. (1927). *Z. Phys.* **44**, 455–472.
 Hume Rothery, W. & Raynor, G. V. (1954). *Structure of Metals and Alloys*. London: Institute of Metals.
 Jena, A. K. & Chaturvedi, M. C. (1984). *J. Mater. Sci.* **19**, 3121–3139.
 Jolly, W. L. (1991). *Modern Inorganic Chemistry*, 2nd ed. New York: McGraw-Hill.
 Kameswari, V. L. (2008). PhD thesis, School of Physics, University of Hyderabad, Hyderabad, India.
 Kameswari, V. L., Seshubai, V. & Rajasekharan, T. (2010). *J. Alloys Compd.* **508**, 55–61.
 Laves, F. (1966). *Intermetallic Compounds*, edited by J. H. Westbrook, pp. 129–143. New York: John Wiley and Sons.
 Lewis, G. N. (1916). *J. Am. Chem. Soc.* **38**, 762–785.

- Machlin, E. S. (1986). *Encyclopedia of Materials Science and Engineering*, Vol. 1, edited by M. B. Bever, p. 395. Oxford: Pergamon.
- Machlin, E. S. & Loh, B. (1980). *Phys. Rev. Lett.* **45**, 1642–1644.
- Marchi, M., Azadi, S. & Sorella, S. (2011). *Phys. Rev. Lett.* **107**, 086807.
- Massalski, T. B. (1990). Editor in Chief. *Binary Alloy Phase Diagrams*, 2nd ed. (plus updates on CD). ASM International, Materials Park, OH 44073, USA.
- Miedema, A. R. (1992). *Physica B*, **182**, 1–17.
- Miedema, A. R., Boom, R. & de Boer, F. R. (1975). *J. Less Common Met.* **41**, 283–298.
- Miedema, A. R., de Chatel, P. F. & de Boer, F. R. (1980). *Physica B*, **100**, 1–28.
- Mohallem, J. R., Vianna, R. O., Quintao, A. D., Pavao, A. C. & McWeeny, R. (1997). *Z. Phys. D*, **42**, 135.
- Mooser, E. & Pearson, W. B. (1959). *Acta Cryst.* **12**, 1015–1022.
- Nissenbaum, D., Spanu, L., Attacalite, C., Barbiellini, B. & Bansil, A. (2009). *Phys. Rev. B*, **79**, 035416.
- Pauling, L. (1929). *J. Am. Chem. Soc.* **51**, 1010–1026.
- Pauling, L. (1950). *Proc. Natl Acad. Sci.* **36**, 533–538.
- Pauling, L. (1975). *The Nature of the Chemical Bond*, 3rd ed. Ithaca: Cornell University Press.
- Pauling, L. (1987). *Proc. Natl Acad. Sci. USA*, **84**, 4754–4756.
- Pearson, W. B. (1962). *J. Phys. Chem. Solids*, **23**, 103–108.
- Pearson, W. B. (1967). *A Handbook of Lattice Spacings and Structures of Metals and Alloys*. Oxford: Pergamon Press.
- Pearson, W. B. (1968). *Acta Cryst.* **B24**, 1415–1422.
- Pearson, W. B. (1972). *The Crystal Chemistry & Physics of Metals & Alloys*. New York: Wiley-Interscience.
- Pettifor, D. G. (1986). *J. Phys. C*, **19**, 285.
- Rajasekharan, T. & Girgis, K. (1983a). *Phys. Rev. B*, **27**, 910–920.
- Rajasekharan, T. & Girgis, K. (1983b). *J. Less Common Met.* **92**, 163–165.
- Rajasekharan, T. & Seshubai, V. (2010a). *Intermetallics*, **18**, 666–671.
- Rajasekharan, T. & Seshubai, V. (2010b). *J. Mater. Res.* **26**, 1539.
- Sauthoff, G. (1996). *Materials Science and Technology*, edited by R. W. Cahn, P. Haasen & E. J. Krammer, pp. 646–766. Weinheim: VCH.
- St John, J. & Bloch, A. N. (1974). *Phys. Rev. Lett.* **33**, 1095–1098.
- Villars, P. & Calvert, L. D. (1985). *Pearson's Handbook of Crystallographic Data for Intermetallic Phases*. Ohio: American Society for Metals.
- Villars, P. & Hulliger, F. (1987). *J. Less Common Met.* **132**, 289–315.
- Walle, A. van de, Ghosh, G. & Asta, M. (2007). *Applied Computational Materials Modeling*, edited by G. Bozzolo, R. D. Noebe, P. B. Abel & D. R. Vij, pp. 1–34. New York: Springer.
- Watson, R. E. & Bennett, L. H. (1978). *Phys. Rev. B*, **18**, 6439–6449.
- Zunger, A. (1980). *Phys. Rev. Lett.* **44**, 582–586.